Treatment Efficacy and Molecular Dynamics of Neoadjuvant Durvalumab and Olaparib in Resectable Urothelial Bladder Cancer: The NEODURVARIB Trial

Juan F. Rodríguez-Moreno[1,2], Guillermo de Velasco[3], Carlos Álvarez-Fernández[4], Ricardo Collado[5], Ricardo Fernández[6], Sergio Vázquez[7], Juan A. Virizuela[8], Pablo Gajate[9], Albert Font[10], Nuria Lainez[11], Elena Sevillano-Fernández[1,2], Osvaldo Graña-Castro[2], Luis Beltrán[12], Rodrigo Madurga[13], Cristina Rodríguez-Antona[14], Pedro Berraondo[15,16,17], Sergio Ruiz-Llorente[2,18,19], and Jesús García-Donas[1,2]

ABSTRACT

Purpose: Neoadjuvant treatment of bladder cancer is evolving, with immunotherapy demonstrating promising activity. PARP inhibition combined with immune activation has been proposed as a synergistic strategy. We conducted a comprehensive molecular characterization of tumors treated with this combination in the neoadjuvant setting to provide crucial results for rational development.

Patients and Methods: A phase II clinical trial was designed to evaluate the combination of anti-PDL1 inhibitor durvalumab and PARP inhibitor olaparib, focusing on biomarker dynamics in both pre- and post-treatment settings. A total of 29 patients were enrolled. Genomic and transcriptomic profiling, as well as analyses of immune cell populations, was conducted at baseline and at the time of cystectomy.

Results: Of the 29 patients treated, a pathologic complete response was observed in 13 cases (44.8%). No major safety concerns were associated with the treatment, and 26 patients (90%) underwent cystectomy. Mutational patterns, tumor mutation burden, and homologous recombination deficiency remained stable throughout treatment and were not predictive of outcomes. However, a shift toward stromal phenotypes and increased expression of epithelial–mesenchymal transition signatures were observed following therapy, particularly in resistant tumors. Moreover, an increase in circulating $CD4^+$ $CD27^-$ $CD28^-$ T cells was noted among responders.

Conclusions: The combination of neoadjuvant durvalumab and olaparib shows therapeutic activity in bladder cancer. Resistance mechanisms seem to be driven by transcriptional adaptations rather than the emergence of new mutations.

Introduction

Systemic treatment in the perioperative setting of muscle-invasive bladder cancer (MIBC) represents a real opportunity to modify the natural history of the disease. Previous trials established the life-prolonging effect of neoadjuvant cisplatin-based chemotherapy (1). In addition, recently published results of the NIAGARA trial showed that the addition of perioperative durvalumab to neoadjuvant chemotherapy significantly improves event-free and overall survival (OS; ref. 2). Immunotherapy has shown consistent efficacy in advanced disease combined either with chemotherapy (3) or enfortumab vedotin (4) as maintenance and in the second or later lines (5–7). Whereas promising phase II studies have been communicated with immune checkpoint inhibitors (CPI), as single agents or in combination with chemotherapy in neoadjuvant therapy (8, 9), pathologic complete response rates (pCRR), a possible surrogate for long-term efficacy, remain around 30% to 40%, similar to chemotherapy alone (10, 11). Interestingly, neoadjuvant clinical trials are incorporating comprehensive molecular analyses to predict response to therapy. Some of them, like COXEN or ABACUS, have

[1]Instituto de Investigación Sanitaria HM Hospitales, Madrid, Spain. [2]Department of Basic Medical Sciences, Institute of Applied Molecular Medicine (IMMA), Facultad de Medicina, Universidad San Pablo CEU, CEU Universities, Urbanización Montepríncipe, Madrid, Spain. [3]Hospital Universitario 12 de Octubre, Madrid, Spain. [4]Medical Oncology Service, Hospital Universitario Central de Asturias, Oviedo, Spain. [5]Complejo Hospitalario de Cáceres, Cáceres, Spain. [6]Medical Oncology Department, Hospital Universitario de Cruces, Barakaldo, Spain. [7]Hospital Universitario Lucus Augusti, Lugo, Spain. [8]Hospital Universitario Virgen Macarena, Sevilla, Spain. [9]Hospital Universitario Ramón y Cajal, Madrid, Spain. [10]Instituto Catalán de Oncología (ICO), Badalona, Spain. [11]Complejo Hospitalario de Navarra, Pamplona, Spain. [12]Department of Cellular Pathology, Barts Health NHS Trust, London, United Kingdom. [13]Faculty of Experimental Sciences, Universidad Francisco de Vitoria, Madrid, Spain. [14]Spanish National Cancer Research Center, Madrid, Spain. [15]Program of Immunology and Immunotherapy, CIMA Universidad de Navarra, Pamplona, Spain. [16]Navarra Institute for Health Research (IDISNA), Pamplona, Spain. [17]Centro de Investigación Biomédica en Red de Cáncer (CIBERONC), Madrid, Spain. [18]Laboratory of Innovation in Oncology, HM CIOCC MADRID (Centro Integral Oncológico Clara Campal), Hospital Universitario HM Sanchinarro, HM Hospitales, Madrid, Spain. [19]Departamento de Biomedicina y Biotecnología, Área de Genética, Universidad de Alcalá, Alcalá de Henares, Spain.

Clinical trial registration ID: NCT03534492

Corresponding Authors: Jesús García-Donas, 1 Gynecological, Genitourinary and Skin Cancer Unit, HM CIOCC MADRID (Centro Integral Oncológico Clara Campal), Hospital Universitario HM Sanchinarro, HM Hospitales, Calle Oña, 10, Madrid 28050, Spain. E-mail: jgarciadonas@hmhospitales.com; and Sergio Ruiz-Llorente, Department of Biomedicine and Biotechnology, Genetics Area, Universidad de Alcalá, Campus Universitario. Ctra. Madrid-Barcelona km. 33, Alcalá de Henares, Madrid 28805, Spain. E-mail: sergio.ruizl@uah.es

Clin Cancer Res 2025;31:1644–56

doi: 10.1158/1078-0432.CCR-24-2890

Translational Relevance

The inclusion of detailed molecular studies in the context of neoadjuvant clinical trials is crucial for identifying both therapeutic response markers and potential mechanisms of resistance. In this regard, the present phase II clinical trial includes the perioperative administration of immunotherapy (durvalumab) and PARP inhibitors (olaparib) in advanced urothelial carcinomas, a combination that has shown therapeutic efficacy in these and other solid tumors. In parallel, our study evaluates comprehensive genomic, transcriptomic, and immune profiles of both transurethral-resected and cystectomy samples, which has allowed us to confirm the activity of such combinations of inhibitors and demonstrate that the biological changes underlying therapeutic resistance are predominantly transcriptomic. However, the genomic and immune alterations resulting from neoadjuvant treatment or associated with the degree of therapeutic response are negligible.

even prespecified biomarkers as primary or coprimary endpoints (12, 13).

Additionally, homologous recombination deficiency (HRD) has been studied across different tumor types as a common hallmark of cancer. Homologous recombination is the most important DNA repair pathway for properly repairing double-strand breaks. PARP inhibitors (PARPi), such as olaparib, are primarily effective in HR-defective tumors and have become a successful targeted therapy (14, 15). PARP inhibition promotes the accumulation of DNA damage in HRD tumors, leading to cell death through synthetic lethality. It is worth mentioning that HRD is present in a subset of bladder cancers and has been associated with leukocyte infiltration, lymphocyte fraction, and an immune-sensitive microenvironment (16, 17). Also, results from trials assessing the combination of durvalumab and olaparib suggest a possible synergy due to an immunogenic modulation, mediated by the STING pathway, along with increased neoantigen production (18). Three randomized clinical trials (BAYOU, ATLANTIS, and Meet-URO 12) have assessed the efficacy of PARPis alone or in combination with immunotherapy in advanced bladder cancer (19–21). Though overall activity was modest, the results improved in cases selected based on their molecular alterations. Similarly, the BISCAY trial showed a modest trend toward a better response rate with durvalumab plus olaparib compared with durvalumab alone in a cohort of patients with HRD (ref. 22). Even so, the ATLAS trial did not find a relationship between HRD status and the efficacy of rucaparib (23). Unfortunately, the definition of HRD varies, with some authors adopting different genetic scores and others focusing on HR repair gene mutations.

Thus, understanding how bladder cancer evolves when exposed to a combination of immunotherapy plus PARPi could be an efficient strategy to integrate these drugs in the management of bladder cancer. With this scope, we designed a phase II clinical trial to assess the impact of neoadjuvant treatment with the combination of durvalumab plus olaparib on the molecular profile of MIBC. Efficacy and safety outcomes were also assessed as secondary objectives.

Patients and Methods

Study design

NEODURVARIB was designed as a multicenter phase II clinical trial and was registered in ClinicalTrials.gov (NCT03534492) prior to its start. The study was conducted in accordance with CONSORT guidelines and was sponsored by the Spanish Oncology Genito-Urinary Group [SOGUG-2017-AIEC(VEJ)-2]. The study population included patients with T2 to T4a bladder cancer aimed for radical cystectomy and eligible for systemic neoadjuvant therapy during 6 to 8 weeks. Subjects eligible for cisplatin were included as determined by the investigators. Adjuvant treatment after cystectomy was allowed based on local clinical practice. Because molecular evolution of tumors was the primary objective of the study, rather than efficacy, cases with nodal involvement were accepted as long as a radical cystectomy was scheduled as part of the clinical management. The main exclusion criteria were concurrent immunosuppressive medication and relevant contraindications for immunotherapy. The primary objective of this study was to assess the impact of neoadjuvant therapy with durvalumab plus olaparib on the molecular profile of resectable urothelial bladder cancer. To achieve this, mutational profiles and gene expression patterns were compared before and after treatment. Secondary objectives included assessing the efficacy of the study combination in terms of pathologic response and radiologic response (based on RECIST 1.1 criteria), determining the impact of molecular alterations on bladder cancer cases, and establishing the toxicity profile of this combination. Other exploratory translational objectives included studying predictive and prognostic biomarkers in tumor tissue and plasma samples, as well as advancing our understanding of this disease and the role of immunotherapy.

Ethical and regulatory considerations

The study was performed in accordance with the ethical principles of the Declaration of Helsinki and was consistent with the International Council on Harmonisation of Technical Requirements for Registration of Pharmaceuticals for Human Use (ICH)/Good Clinical Practice. The study protocol was approved by the Ethics Committee and Spanish regulatory authorities. Every patient provided written informed consent prior to enrollment.

Sex as a biological variable

Despite urothelial carcinoma being more prevalent in men than in women, sex has not been considered a biological variable of interest, assuming that the molecular mechanisms underlying its progression and the therapeutic efficacy of the inhibitors used in this clinical trial are not influenced by sex.

Treatment protocol

The subjects received two cycles of treatment for up to a maximum of 2 months, unless there was unacceptable toxicity, withdrawal of consent, or another discontinuation criterion. A fixed dose of 1,500 mg of durvalumab (MEDI4736) via intravenous infusion was administered on days 1 and 29 every 4 weeks (Q4W). Olaparib was administered orally twice a day at 300 mg for 8 weeks. Cystectomy was scheduled to be performed after these two cycles but could be conducted after the sixth week of treatment, as determined by the investigator. Olaparib was required to be discontinued at least 7 days prior to cystectomy. All patients had safety assessments performed every cycle (cycle 2 day 1 and before cystectomy) and 28 days after treatment discontinuation. No additional follow-up was conducted.

Statistical analysis for determination of sample size

We adopted the Fleming model to calculate sample size. Based on this model for a one-stage phase II trial, with a probability of type I

error (α) = 0.05 and power ($1 - \beta$) = 0.8, setting up the lower proportion for rejection (p0) = 0.2 and higher proportion for acceptance (pn) = 0.40, the sample size required for this trial was 29 patients.

Statistical methods

Categorical data were summarized in tables presenting frequencies and percentages. Continuous data were summarized using the mean, median, SD, and range. The number of nonevaluable outcomes and of missing data was also provided. The exact 95% confidence interval (CI) of the response rate was included. Toxicity was described per patient to show all the adverse event (AE) information, including severity and relationship with the study treatment. AEs were evaluated according to the NCI CTCAE v4.03 criteria, and postoperative complications were considered AEs. The statistical evaluation was performed using the software package IBM SPSS Statistics release version 22 (RRID: SCR_002865).

Efficacy assessments

The pCRR was analyzed based on the percentage of patients who obtained a pCR on cystectomy tumor sample. The number and percentage of subjects falling into each response category were also tabulated. The radiologic response rate was determined by CT/MRI and comparing baseline assessment values with those prior to cystectomy.

Biomarker sampling and evaluation methods

The biological responses to the study treatment were assessed at the Innovation Laboratory in Cancer at the Clara Campal Comprehensive Cancer Center. Archival bladder formalin-fixed, paraffin-embedded (FFPE) tumor blocks, collected as part of the patient's normal clinical care, at the time of transurethral resection of bladder tumor (TURBT) and after the cystectomy surgery, were collected from each patient. Sections of the paraffin-embedded tissue (2–4 μm) were independently assessed by a central pathologist (Pathognomics Ltd.).

Tissue sample processing

Hematoxylin–eosin sections of the paraffin-embedded tissue (2.5 μm) were analyzed by a central pathologist (Pathognomics Ltd.) to confirm histologic type, differentiation grade, tumor content, and presence or absence of vascular invasion. The pathologist also marked tumoral and nontumoral areas for further analysis, which included the extraction of both genomic DNA and total RNA. FFPE blocks were also used to obtain additional 2.5-μm sections, in which immune-related relevant markers were evaluated. In this regard, IHC was used to assess the number and composition of immune infiltrates to define the immune cell subsets present within FFPE tumor tissue before and after exposure to therapy. These IHC analyses included the following markers: CD4, CD8, FOXP3, fibroblast activation protein (FAP), PDL1 (Sp142 clone, Ventana; evaluated either at the tumoral or immune area or as combined scored), granzyme B, and T-cell markers. These slides were assessed by the pathologist of the study to detect positivity on each determination.

Omics studies and subsequent estimation of HR defects, bladder carcinoma subtyping, and immune populations

The extraction of nucleic acids from paraffin-embedded samples enabled the identification of point mutations and chromosomal alterations in the samples under study through massive exome sequencing, as well as significant variations in gene expression via RNA sequencing (RNA-seq). Subsequent genomic data analysis facilitated the identification of potential alterations in variables associated with HR defects (ScarHRD package): loss of heterozygosity (LOH), telomeric allelic imbalances (TAI), and large-scale transitions (LST; ref. 24). Additionally, transcriptomic results allowed for the determination of the urothelial carcinoma subtype (BLCAsubtyping; ref. 25) and the identification of potential immune system components altered in the comparisons of interest (Cibersort; RRID: SCR_016955; ref. 26).

Whole-exome sequencing

In brief, whole-exome sequencing (WES) was performed using tumor DNA isolated from FFPE tissues and using as a reference DNA isolated from normal tissue of the same patient or peripheral blood (Novogene). About 5 to 10 μg of DNA was needed from each sample. After DNA fragmentation, whole-exome capture was performed using SureSelect Agilent Technology (Human All Exon V6, Agilent Technology). Library size and concentration were determined using Bioanalyzer 2100 (Agilent Technology), and exome sequencing was performed at a median coverage of 200× using 150-bp paired-end technology in a HiSeq2000 system (Illumina). Illumina's Real-Time Analysis software was used for image analysis and the base calling, and the programs GEM and BFAST were used for aligning the sequences of the human genome. The identification of single-nucleotide variants (SNV) and indels was performed with the program SAMtools. Variants filtering, selection of candidates, and data analysis were performed in a similar way, based on our prior experience with these kinds of studies. The WES data generated in this study are uploaded to the European Genome–Phenome Archive (EGA) and are available under the accession number EGAC50000000471.

ScarHRD package

HRD-related scores, including TAIs, LOH, number of LSTs, and its combined score (HRD score) were estimated using scarHRD R package (https://github.com/sztup/scarHRD; ref. 24), which determines the levels of HRD based on next-generation sequencing, with either WES or whole-genome sequencing data.

RNA-seq

RNA-seq libraries were constructed and sequenced on an Illumina HiSeq PE150 platform with 150-bp paired-end reads (Novogene). After the quality control procedures, mRNA from eukaryotic organisms was enriched using oligo(dT) beads, and rRNA was removed using the Ribo-Zero kit. Once random mRNA fragmentation and cDNA synthesis by using mRNA template and random hexamers primer were performed, a customized second-strand synthesis buffer (Illumina), dNTPs, RNase H, and DNA polymerase I were added to initiate the second-strand synthesis. Following several steps which included terminal repair, a ligation and sequencing adaptor ligation, the double-stranded cDNA library was completed through size selection and PCR enrichment, and several quality control processes (Qubit 2.0, Agilent 2100 Bioanalyzer and Q-PCR). The qualified libraries were fed into Illumina sequencers after pooling according to its effective concentration and expected data volume.

First-strand 150 bp paired-end reads were analyzed with the Nextpresso (27) pipeline as follows: sequencing quality was checked with FastQC v0.11.0 (RRID: SCR_014583). Reads were aligned to the human genome (GRCh38) with TopHat2 (RRID: SCR_013035; ref. 28) using Bowtie1 (29) and Samtools (RRID: SCR_002105; ref.

30), allowing 4 mismatches and 20 multihits. The GENCODE v36.GRCh38. Ensembl_102 gene annotation was used (RRID: SCR_014966; ref. 31). Read counts were obtained with HTSeq (RRID: SCR_005514; ref. 32). Differential expression and normalization were performed with DESeq2 (RRID: SCR_000154; ref. 33), keeping only those genes with more than 2 normalized counts in at least 30% of the samples. Finally, those genes that had an adjusted *P* value below 0.05 FDR were selected. GSEAPreranked (RRID: SCR_003199; ref. 34) was used to perform gene set enrichment analysis (GSEA) to evaluate the potential implication of certain biological processes. Gene signatures were obtained from the Molecular Signatures Database (35), KEGG pathways (C2), cancer hallmarks (H), oncogenic signatures (C6), ontology gene sets (C5), and immunologic (C7) and chromosome (C1) locations (RRID: SCR_012773). Only those gene sets with significant enrichment levels (FDR q-value < 0.25) were considered. Raw and processed RNA-seq data are publicly available from the Gene Expression Omnibus (RRID: SCR_005012) database with the ID GSE225066.

Identification of components of the immune system

We used Cibersort analytical tool (RRID: SCR_016955) to impute gene expression profiles and provide an estimation of the abundances of different cell types derived from the immune system (NK cells, naïve and memory B cells, myeloid subsets, plasma cells, and T-cell types, among others) in a mixed cell population (36).

Transcriptomic classifier

BLCAsubtyping *in silico* tool was used to classify our cohort of bladder carcinomas according to six previously published classification systems [Baylor College of Medicine, University of North Carolina, MD Anderson Cancer Center, Lund University, The Cancer Genome Atlas (TCGA) consortium, and Cit-Curie]. These classifiers were merged into an R package (R Foundation for Statistical Computing) that is documented and freely available at https://github.com/cit-bioinfo/BLCAsubtyping (25).

Flow cytometry analyses and sorting of immune-related cells

Blood extractions were performed before initiating treatment (cycle 1 day 1), 4 weeks later (cycle 2 day 1), the day of cystectomy (before surgery), and 4 weeks later (follow-up; Supplementary Fig. S1). Ten milliliters of peripheral blood was collected in 10-mL heparin-containing tubes and mixed with 10 mL of ice-cold PBS. The cell suspension was laid over 15 mL of Ficoll-Hypaque (GE Healthcare Europe GMBH) gradients in 50-mL tubes and centrifuged at 2,200 rpm for 20 minutes at 20°C. The leukocyte layer was resuspended in 5 mL ice-cold PBS. Subsequently, cells were stained with fluorochrome-conjugated mAbs (Supplementary Table S1). Stained cells were analyzed using a FACSCanto flow cytometer (Beckman Coulter). FlowJo software (RRID: SCR_008520; TreeStar) was applied for data analysis, and fluorescence minus one controls were used.

Data availability

Qualified scientific and medical researchers may request molecular data underlying the results reported in this article, following deidentification. Data requests will be evaluated and approved by the co-corresponding authors. Omics raw data from this study are publicly available in the Gene Expression Omnibus database (RNA-seq; RRID: SCR_005012) with the ID GSE225066 and the EGA (WES, RRID: SCR_004944) under the accession number EGAC50000000471. Both datasets are accessible upon reasonable request from the corresponding author.

Results

Patient demographics

Between November 2018 and October 2019, 39 eligible patients were identified, of whom 29 ultimately enrolled. Reasons for screening failure included the decision to proceed with cystectomy without neoadjuvant treatment in five patients (50%), as well as nonmeasurable disease, active infection, patient unwillingness to comply with protocol procedures, renal insufficiency, and altered laboratory tests in one case each (10%; Supplementary Fig. S2). Demographic characteristics are summarized in **Table 1**, and representativeness of the study participants is shown in Supplementary Table S2. Twenty-six (90%) patients were male. Seventeen (59%) had an Eastern Cooperative Oncology Group performance status (ECOG-PS) of 0, and 12 (41%) had an ECOG-PS of 1. The median age was 69 years (range, 43–85). Tumor staging revealed T2 in 23 (79%) patients, T3 in 4 (14%), and T4 in 2 (7%). Additionally, nodal spread was observed in four patients (13%). One case was deemed N2, one N3, and one M1a, with one case considered N-positive without specifying the category. Twenty-five (86%) had pure urothelial cancers, whereas 4 (14%) presented mixed histology with a squamous component. Three (10%) patients had a history of prior non-MIBC.

Clinical outcomes and analysis

Radiologic response was evaluable in 25 cases, resulting in an overall response rate of 28% [95% CI, (10.4%–45.6%)]. Stable disease was observed in 15 patients (60%), yielding a clinical benefit rate of 88% [95% CI, (75.3%–100%)]. Disease progression was deemed as the best tumor response in three cases (12%; **Table 2**). Among the 29 patients treated, a pCR was observed in 13 cases [44.8%; 95% CI, (31.9%–68.1%)]. None of the three cases that experienced progression during treatment underwent bladder resection.

The median time on treatment was 7 weeks (range, 0.3–9.4), with the majority of patients (93.1%) receiving two neoadjuvant cycles (Supplementary Tables S3A and S3B). Temporary interruptions occurred in four cases (14%) due to hematuria, exacerbation of chronic obstructive pulmonary disease, febrile syndrome, and diarrhea, with one case each (Supplementary Table S3C). Grade 3 toxicity (neutropenia) was observed in 3.4% of patients, which was deemed to be related to the study drugs (Supplementary Table S4). The safety profile was manageable, with no unexpected AEs, no need for olaparib dose reduction, and no surgery delays due to toxicity. Discontinuation of combination treatment was necessary in two cases, one due to sepsis and another due to grade 3 chronic obstructive pulmonary disease exacerbation (Supplementary Table S5). Four cases (14%) experienced postoperative complications, including two cases of grade 3 wound eviscerations and two deaths. All complications were deemed unrelated to the study treatment.

Molecular assessments

Samples for assessing the impact of neoadjuvant treatment with durvalumab plus olaparib on the molecular profile of resectable urothelial bladder cancer (the primary endpoint of the study) were available from TURBT in 29 cases and from cystectomy in 26. A comprehensive IHC panel analysis, WES, and RNA-seq were

Table 1. Patient demographics.

			Median	Range
Age			69	43–85
			Value %	
Gender	Males		26	90
Race	Caucasian		29	100
Eastern Cooperative Oncology Group performance status	0		17	59
	1		12	41
Histology	Transitional		25	86
	Mixed (squamous)		4	14
Tumor–node–metastasis	Tumor	2a	13	45
		2b	10	34
		3a	4	14
		4a	2	7
	Node	0	15	52
		1	3	10
		2	1	3
		X	9	31
		NA	1	3
	Metastasis	0	23	79
		1	1	3
		Mx	4	14
		NA	1	3
	Stage	I	1	3
		II	15	52
		IIIA	5	17
		IIIB	2	7
		IVa	3	10
		NA	3	10

performed. Peripheral blood samples were obtained from 29 patients for flow cytometry analysis of circulating immune cells. Sample collection was scheduled on day one of both treatment cycles, at the time of surgery, and 4 weeks after cystectomy (follow-up visit; Supplementary Fig. S1). Cases were categorized as responders or nonresponders based on the achievement of a pCR.

IHC

Considering the administration of durvalumab in the neoadjuvant setting in our trial and the therapeutic potential associated with other immune checkpoint inhibitors in previous clinical trials, we evaluated the expression levels of various markers related to the main immune system populations. We then correlated these levels with potential changes between the study samples (TURBT vs. cystectomies) or with the degree of response at baseline. Whereas nonsignificant changes were observed for FOXP3, PDL1 combined positive score (CPS), and PDL1 at immune component, FAP and PDL1 staining significantly increased in tumoral cells after the administration of the combination of durvalumab plus olaparib ($P = 0.049$ and $P = 0.009$, respectively; **Fig. 1A**; Supplementary File S1). In contrast, we observed higher expression of markers related to T cell–mediated response (CD4 and CD8) in the diagnostic samples, with these changes being significant for CD4 ($P = 0.006$) and showing a statistical trend for CD8 (P value $= 0.08$; **Fig. 1A**; Supplementary File S1).

The inclusion of a representative number of patients diagnosed with squamous cell carcinomas (SCC; $n = 4$) in our study allowed us to evaluate whether the expression of these immune markers showed differential patterns between this histology subtype and the conventional urothelial carcinoma ($n = 25$). In this case, we observed notable differences in the PDL1 CPS, which was significantly higher for SCCs (P value $= 0.002$; **Fig. 1B**). Only one of these four cases presented a CPS < 10 at baseline and reported disease progression as the best response (**Fig. 1B**). Thus, all three cases with a squamous component and CPS > 10 achieved a pCR.

Finally, we evaluated whether the expression values of these markers in the baseline TURBT samples correlated to any extent with the clinical response of the patients under study, categorizing them as nonresponders and responders. In this regard, no difference was observed between those groups regarding PDL1, FAP, CD8, CD4, FOXP3, or granzyme B staining (**Fig. 1C**). Staining scores for these immune markers are available as Supplementary Materials (Supplementary File S1).

WES

From a genomic perspective, we decided to characterize the most frequent point mutations and genomic alterations in our cases by performing WES on both diagnostic and surgical samples. The analysis of the results demonstrated a high sequencing depth (average 229×)

Table 2. Radiologic response, RECIST 1.1 criteria.[a]

Radiologic response	*N*	%
Partial response	7	28
Stable disease	15	60
Progressive disease	3	12
Total	25	100

[a]Determined in 25 cases with complete assessment of response.

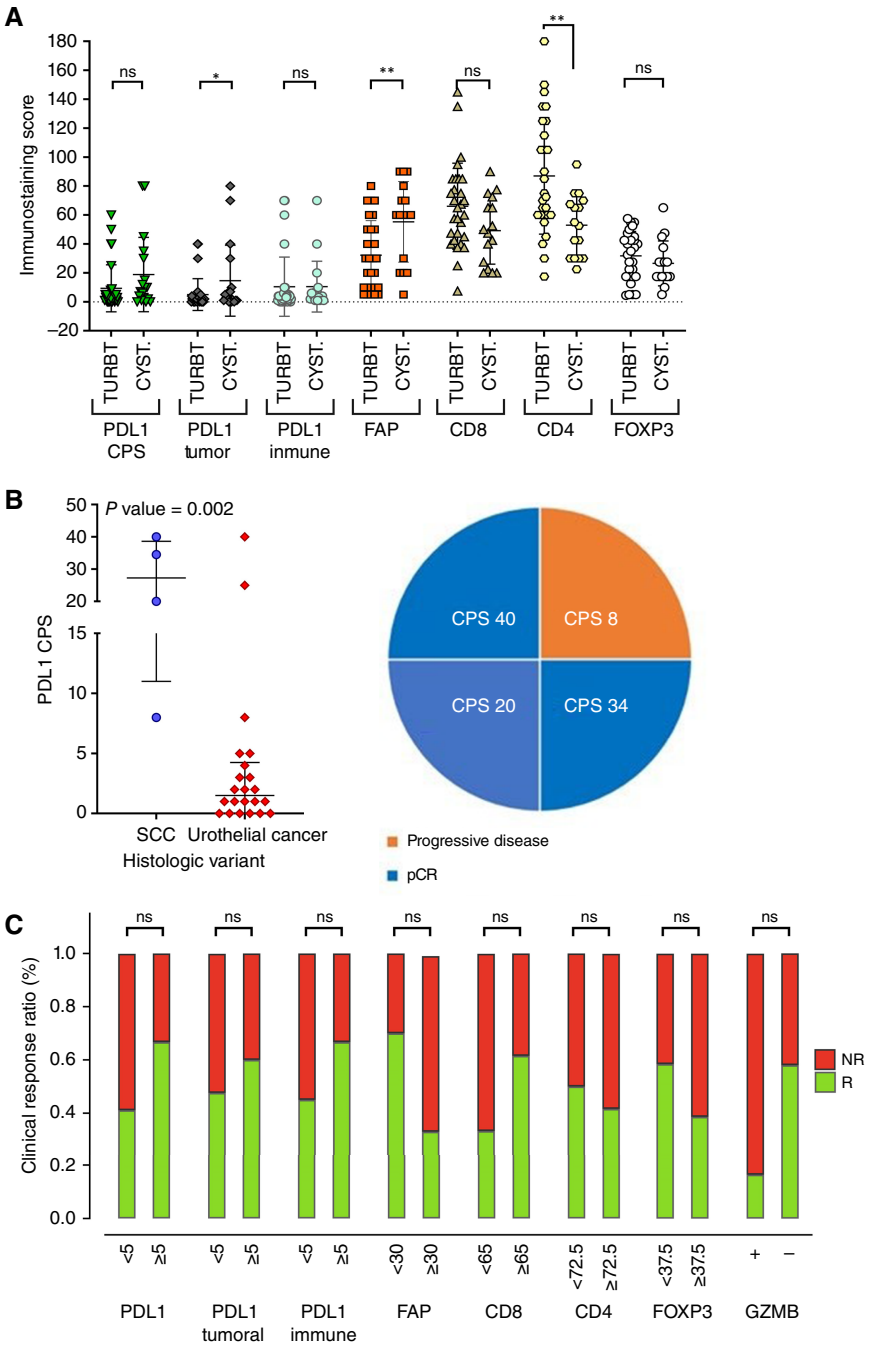

Figure 1.

IHC profiling of samples under study. **A,** IHC patterns at baseline TURBT compared with cystectomy (CYST). PDL1 staining was assessed as the CPS but also in tumor cells (tumor) and immune cells separately (noted as "PDL1 tumor" and "PDL1 immune," respectively). Mann–Whitney U test. **B,** Comparison of the median CPS between tumors with a squamous component (SCC) and pure urothelial cancers (Mann–Whitney U test) and sectorial graph depicting the response to treatment (blue: pCR; orange: progressive disease). Numbers represent the CPS. **C,** Percentage of patients who achieved a clinical response (green bars) vs. those who did not (red bars), classified by the positive or negative expression of different IHC markers in the baseline (TURBT) sample [PDL1, PDL1 in tumor cells, PDL1 in immune cells, FAP, CD8, CD4, FOXP3, and granzyme B (GZMB); Fisher *t* test]. NR, nonresponder; R, responder. Degrees of statistical significance: ns, nonsignificant; *, $P < 0.05$; **, $P < 0.01$.

and a high percentage of correctly mapped reads (>99%), with an average of 124 million sequences per sample (Supplementary File S2). Notably, the percentage of mutations detected in genes frequently altered in our urothelial carcinoma baseline setting was similar to that described in previous seminal works (TCGA consortium and ABACUS study; refs. 37, 38; Supplementary Files S3 and S4).

Given that the anatomopathologic evaluation of radical cystectomy tissue from certain patients with complete radiologic response identified areas containing a residual percentage of tumor cells compared with the proportion of other tissue components, we decided to also perform WES on cystectomy tissues from responder patients. Although genomic profiling of these regions revealed common profiles between diagnostic and cystectomy samples (**Fig. 2A**) in responders (especially for samples ID#2 and #17), the ratio of allele frequencies (cystectomy/TURBT) of different variants detected in these genes previously associated with the development of urothelial cancer decreased dramatically in responders (0.3-fold change). However, in nonresponders, the allele frequencies remained stable (1.1-fold change), representing statistically significant differences between the groups (**Fig. 2A**). Consistent

with these findings, we also observed a greater reduction in the total number of concordant alterations comparing responders versus nonresponders ($P < 0.0005$, **Fig. 2B**), which would support a relationship between the molecular findings and the radiographic responses observed in responders. This behavior was also evident when comparing the mutational profiles of the 29 most frequently altered genes in bladder cancer, as reported by TCGA (**Fig. 2C**; ref. 37). Globally, these data also indicated a significant reduction in the fraction of tumoral cells in surgical specimens from responders and confirmed the clinical response of patients from a molecular perspective.

Tumor mutational burden (TMB) and HRD, determined as a composite score including LOH, TAIs, and LSTs, remained unchanged between TURBT and cystectomy (**Fig. 2D** and **E**). Additionally, no differences were observed between baseline samples in responders and nonresponders in terms of mutational patterns, TMB, or HRD (Supplementary Fig. S3A and S3B).

Considering the biological relationship between the presence of defects in genes related to HR in solid tumors and the clinical response of these neoplasms to PARPis, we compared the presence of pathologic variants in the BROCA gene set according to the clinical response and the mutational status of our cohort. This panel has been widely used as an indirect assessment of HRD and comprises 84 HR-related genes harboring actionable mutations detected in breast and ovarian carcinomas. In this regard, there was no difference in the number of BROCA mutations considering the clinical response (responders vs. nonresponders; Supplementary File S3). However, a positive correlation was observed between TMB and the number of variants affecting BROCA-related *loci* (Supplementary Fig. S3C). This association reached statistical significance when comparing wild-type tumors versus tumors harboring *BRCA1* or *BRCA2* mutations ($P < 0.001$; Supplementary Fig. S3D; Supplementary File S3).

Overall, the results obtained from the WES reflect that these tumors do not undergo significant genomic alterations as a consequence of the neoadjuvant treatment. Additionally, the genomic variables under study were unable to predict the degree of clinical response in the patients.

Gene expression comprehensive profiling

The transcriptomic studies were conducted on a total of 26 samples, including 16 collected prior to neoadjuvant treatment. To identify potential molecular categories associated either with the treatments used (cystectomy vs. TURBT) or with the clinical response observed in patients (responders vs. nonresponders), we proceeded to analyze the transcriptomic results obtained from both comparisons using GSEA (Supplementary Files S5 and S6). In the comparison between posttreatment samples and baseline samples, we identified 28 enriched categories in posttreatment patients (FDR < 0.25), with 12 of 28 showing a corrected P value < 0.001, **Fig. 3A**), which were predominantly associated with changes in cellular phenotype [epithelial–mesenchymal transition (EMT)] and immune and inflammatory responses (IFN-mediated processes, STAT-IL factors, or TNF). Regarding the enriched pathways in TURBT samples, we primarily observed categories related to cell-cycle regulation (E2F, G2M checkpoint, and *MYC* oncogene; FDR < 0.25; **Fig. 3A**). In identifying molecular signatures associated with patients' therapeutic sensitivity, GSEA analysis revealed statistically significant categories similar to those observed in the comparison between cystectomy and TURBT. It is worth mentioning that enrichment of signatures associated with EMT and immune and inflammatory responses was observed in nonresponding patients (**Fig. 3B**). Conversely, samples from responding patients showed associations with categories related to cell-cycle checkpoint (**Fig. 3B**).

Subsequently, we attempted to identify potential enriched chromosomal regions, either in responding or nonresponding patients, as a result of significant variations in the expression of genes located in these genomic regions. In this regard, responding patients showed greater enrichment of regions located on the long arm of chromosome 13 (FDR < 0.001; **Fig. 3C**), notably the 13q14 band, which includes the *RB1* tumor-suppressor gene. In contrast, nonresponding cases were associated with enrichment of chromosomal regions on the long arm of chromosome 1 (FDR < 0.001), among other areas of interest (**Fig. 3C**). Specifically, a correlation was detected with the 1q23 region, which contains the *DEDD locus*, and the 1q21 region, which includes the *S100A8* and *S100A9* genes, among others. Accordingly, the analysis of differentially expressed genes between responders and nonresponders yielded significant data for both genes (*S100A8*/*S100A9*, $\log_2$ FC: 5.35 and 4.95, adjusted P value: 9.18e−10 and 1.06e−10, respectively; **Fig. 4A**). In the same figure, other differentially expressed genes in the two comparisons of interest are also shown, which, although potentially relevant to disease progression, do not exhibit *a priori* an obvious biological relationship with urothelial carcinoma.

Finally, we compared the mutational patterns obtained through WES for certain genes of interest (*FGFR3* and *TP53*, among others) with the expression levels of functionally related genes (Supplementary Fig. S4A). In this regard, we observed a clear correlation between the presence of alterations in *FGFR3*, whether *TACC*-rearrangements or pathogenic point mutations, and an increase in the expression of its corresponding messenger RNA (Supplementary Fig. S4B, P value < 0.01). In contrast, the presence of inactivating *TP53* mutations was significantly associated with decreased expression of *MDM2*, a well-known negative regulator of TP53 (Supplementary Fig. S4C, P value < 0.005).

Tumor taxonomy

In order to estimate the molecular subtype to which the samples from our study patients belong, we used the *in silico* program "*BLCAsubtyping*" (25). This tool, which allows associating transcriptomic profiles with six different classifiers (Baylor College of Medicine, University of North Carolina, MD Anderson Cancer Center, Lund University, TCGA, and MIBC), demonstrated an almost complete association of alterations in the *FGFR3* locus with the luminal papillary phenotype (MIBC classifier, four of five cases) and a strong correlation between the presence of inactivating *TP53* mutations and the basal/squamous, luminal unstable, and neuroendocrine phenotypes (MIBC classifier, seven cases; **Fig. 4B**). It is also worth noting that of the cases for which we had paired samples (six patients), three showed concordance between the diagnostic sample and the cystectomy (two cases with a basal/squamous phenotype and one classified as neuroendocrine). However, the remaining three patients progressed from an initial unstable luminal or papillary phenotype to a basal/squamous profile in the surgical sample. These findings suggest that the main molecular changes induced in patients as a result of neoadjuvant treatment occur at the transcriptional level.

Immune infiltration in tumor tissue

With the aim of determining to what extent neoadjuvant treatment modified the immune component associated with the tumor in the tumor microenvironment, we utilized Cybersort, an analytical deconvolution tool for expression data to facilitate an estimation of the relative abundance of 22 different immune populations. In this regard, no significant differences were found in these populations

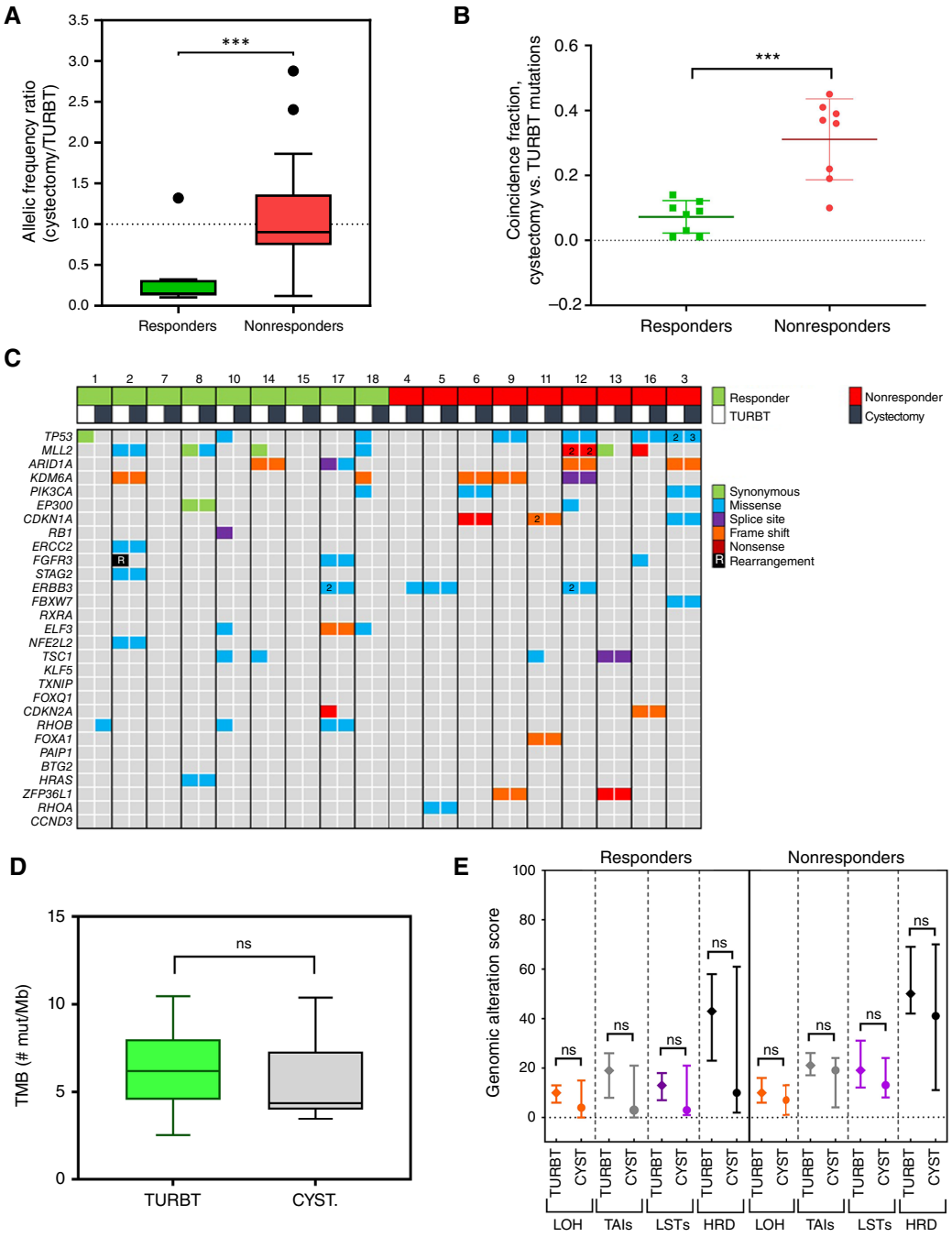

Figure 2.

Genomic profiling comparing TURBT vs. cystectomies. **A,** Box and whisker plot showing the ratio of the allelic frequency of genetic variants in cystectomy samples between the allelic frequency in TURBT samples in responder vs. nonresponder patients (***, $P < 0.001$). **B,** Dot plot showing the fraction of mutations detected by WES that are coincident between the cystectomy and TURBT in responders and nonresponders (***, $P < 0.001$). **C,** Genetic variants detected in our cohort for the 29 most frequently mutated genes according to TCGA in the TURBT and cystectomy samples of responders (marked in green) and nonresponders (marked in red). **D,** Box and whisker plot comparing the TMB in samples from TURBTs vs. cystectomies. **E,** Comparison of the percentage of samples with genomic alterations related to HRDs (LOH, TAIs, LSTs, and HRD score) in TURBT samples vs. cystectomies and in responders vs. nonresponders comparing diagnostic samples and cystectomies. CYST, cystectomy. Degrees of statistical significance: ns, nonsignificant.

either based on the sample (pre- and post-treatment) or based on clinical response (responders vs. nonresponders; Supplementary Fig. S5).

Immune populations in peripheral blood

Concurrently, the systematic collection of peripheral blood from the patients under study at different points of the neoadjuvant

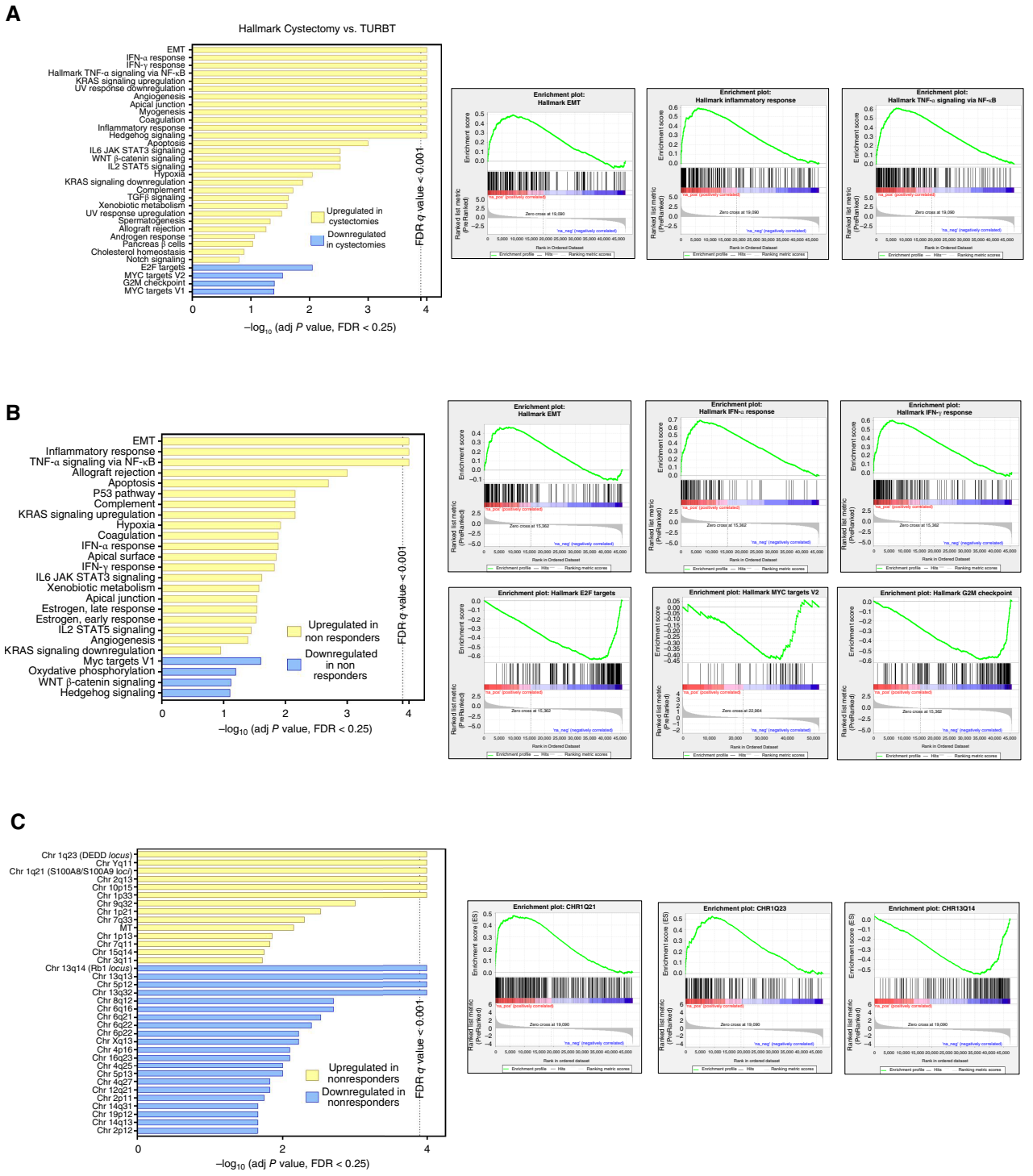

Figure 3.

Functionally enriched categories in transcriptomic studies for the comparisons of interest [baseline samples (TURBT) vs. cystectomies or nonresponders vs. responders]. **A** and **B,** Enriched categories for the Hallmark gene sets (Human MSigDB Collections—GSEA) in samples from cystectomies (posttreatment) vs. TURBTs (baseline). **A,** Enriched categories for the Hallmark gene sets (Human MSigDB Collections—GSEA) in nonresponders compared with responders (**B**). **C,** Enriched categories for the gene set corresponding to human chromosome cytogenetic bands (Human MSigDB Collections—GSEA) in the comparison of nonresponders compared with responders. Yellow bars indicate categories enriched in the study group, whereas blue bars indicate categories enriched in the control group, with a statistical significance of FDR < 0.25 (**A**) or <0.025 (**B** and **C**), respectively. The dashed vertical line reflects an FDR value of <0.001. The GSEA curves for the most significantly enriched categories are shown to the right of the bar graphs.

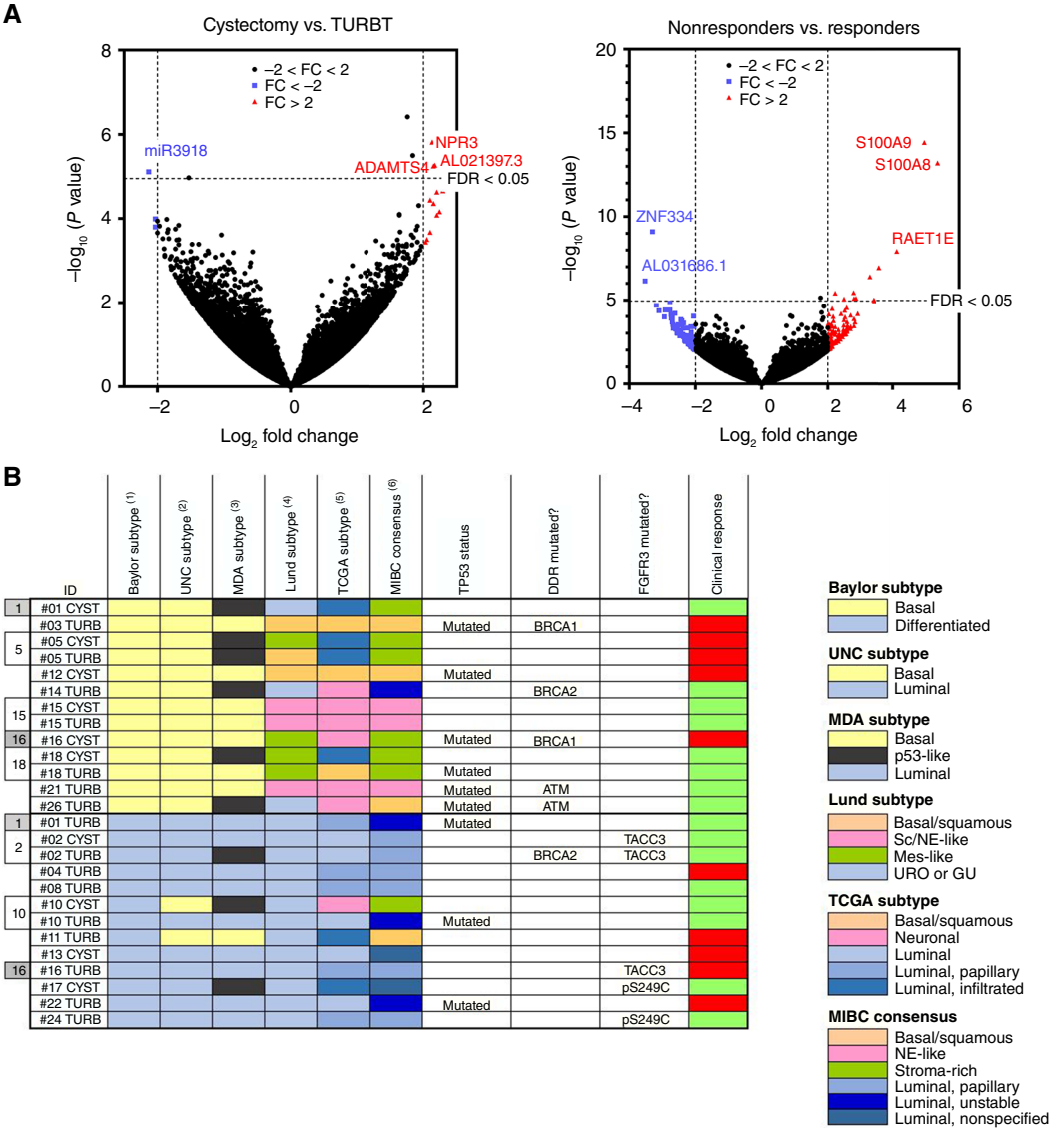

Figure 4.

Analysis of the data obtained from the transcriptomic profiling of the study samples. **A,** Volcano plots showing the transcriptionally deregulated genes in the comparisons of interest, whether comparing cystectomy (posttreatment) samples vs. TURBT (baseline) samples (left) or by response degree (nonresponder vs. responder, right). The horizontal axis shows the $\log_2$ of the fold change, with the vertical dashed lines marking values below −2 or above +2. The vertical axis reflects the $-\log_{10}$ of the *P* value, with the dashed line indicating an FDR value of <0.05. The top left and right quadrants indicate the genes with the greatest changes in fold change and statistical significance. Red circles represent overexpressed genes in the study condition (cystectomy in the left volcano plot and nonresponders in the right volcano plot), whereas blue circles represent overexpressed genes in the control condition (TURBT in the left volcano plot and responders in the right volcano plot). **B,** Panel indicating the molecular subtypes by which the study samples are classified based on their transcriptomic profile. The results shown in this panel were obtained using the *in silico* tool "BLCAsubtyping," allowing their assignment to the various molecular groups previously described and discussed in Kamoun and colleagues (25), which includes classifications from the Baylor College of Medicine (Baylor), University of North Carolina (UNC), MD Anderson Cancer Center (MDA), Lund University (Lund), TCGA consortium, and Kamoun and colleagues' own study (CIT-Curie, MIBC). Additionally, the mutational status of *TP53*, genes related to HR, and *FGFR3* are reflected, along with the sample type [cystectomy (CYST) or TURBT] and patient response grade (green boxes, responders; red boxes, nonresponders). GU, genomically unstable; MES, mesenchymal; Sc/NE, small cell/neuroendocrine-like; URO, urothelial-like.

treatment (Supplementary Fig. S1) aimed to estimate different circulating immune populations and potentially correlate any changes over time with the clinical response of the patients. To this end, comprehensive panels of flow cytometry were designed and applied to determine the percentage and phenotype of different subsets of myeloid cells, effector $CD4^+$ and $CD8^+$ T lymphocytes, and T regulatory cells (Supplementary File S7; Supplementary Table S1), assessing dynamic changes in these immune subsets. No statistical differences were detected between responders and nonresponders in most of the immune populations. Interestingly, $CD4^+$ T

lymphocytes with low expression of CD27 and CD28, indicative of effector memory T cells, showed a trend toward a higher concentration in responders at baseline and increased throughout treatment, reaching statistical significance at follow-up ($P = 0.04$; Supplementary Fig. S6).

Discussion

NEODURVARIB is a phase II clinical trial that assessed the molecular modifications induced by the combination of durvalumab plus olaparib as neoadjuvant treatment in bladder cancer. A pathologic response rate of 44.8% was achieved in 29 cases included in the trial. Although genomic variants remained stable throughout treatment, an increased activation of the EMT signature was observed at the time of cystectomy and in nonresponders Thus, transcriptomic adaptations, rather than genomic alterations, seem to lead to differential clinical outcomes in this disease.

Perioperative treatment in MIBC has been shown to improve OS; therefore, the development of new combinations and the understanding of resistance mechanisms in this scenario have become a priority (1). Three randomized clinical trials have assessed the efficacy of PARPis in advanced bladder cancer (19–21). The BAYOU study compared the combination of durvalumab plus olaparib versus durvalumab plus placebo. Although no difference was observed in the whole study population, cases with homologous recombination repair gene mutations achieved a longer progression-free survival. The ATLANTIS study assessed the role of rucaparib as maintenance therapy in patients with a DNA repair deficiency phenotype. Though recruitment was prematurely stopped due to the approval of avelumab in this setting, a difference in progression-free survival favoring PARPis was reported. However, the ATLAS trial did not find a relationship between HRD status and the efficacy of rucaparib (23). Finally, the Meet-URO 12 trial studied niraparib as maintenance therapy in an unselected population, with no benefit compared with best supportive care. Overall, these results highlight the relevance of improving molecular determinants of sensitivity and resistance to PARPis in bladder cancer.

Based on the proven activity of immunotherapy in metastatic disease and the potential synergy with a PARPi, we designed a phase II trial that aimed to describe the evolution of the molecular alterations of bladder cancers under durvalumab plus olaparib (17). In our series, 13 of 29 eligible cases (45%) achieved a pCR. This is in line with prior studies that have communicated a pathologic response rate of 30% to 40% with both chemotherapy and immunotherapy (alone or in combination; refs. 3, 8, 9). The pathologic response rate is key, as it has been proposed as a surrogate marker of OS (10). However, the relatively small study population in our study and the high percentage of T2 tumors (79%) make comparison with other series challenging. Unfortunately, three patients progressed during neoadjuvant treatment and could not undergo cystectomy as scheduled. These numbers are similar to most neoadjuvant trials, which have communicated progressive disease rates of around 16% to 20% and compliance with cystectomy between 80% and 90% (1, 8, 9, 11).

It is important to highlight that this is an exploratory trial with limitations that should be considered when interpreting the results. The small population and lack of randomization in the design make it difficult to evaluate the efficacy and safety data of the durvalumab and olaparib combination. Additionally, the short follow-up does not allow for the assessment of long-term outcomes or late AEs, which should be explored further.

Regarding the molecular characteristics of tumors at baseline, 9 (34.6%) cases showed PDL1-positive staining. This is similar to other neoadjuvant studies, such as ABACUS, but higher than in trials in the metastatic setting (i.e., Imvigor210; refs. 39, 40). Patients with a SCC component at the initial biopsy showed a significantly higher CPS, and 75% of them achieved a pCR. Interestingly, the only patient who progressed had the lowest CPS (below 10). These results are in line with a prior experience with pembrolizumab within the PURE01 trial, in which eight SCC bladder tumors were included (41). Investigators demonstrated a higher PDL1 expression and mutational load in these tumors. Also, they achieved a higher response rate than urothelial cancer or other subtypes.

In this study, the combination of durvalumab and olaparib significantly increased the expression of PDL1 and FAP. Both proteins have been associated with mechanisms of immune evasion and could reflect a reaction of the tumor and its environment under the pressure of a CPI (42). Though these results could suggest FAP as a potential target in bladder cancer, no differences were observed between responders and nonresponders. On the contrary, CD4 decreased and CD8 presented a similar trend after treatment. Because this change had no impact on the outcome, it could just reflect the hematologic toxicity of olaparib rather than a significant immunosuppression (43).

WES did not show meaningful differences between baseline and posttreatment samples. Mutational patterns, TMB, and HRD score remained stable throughout treatment, and no differences were observed between responders and nonresponders. Although TMB is considered a biomarker of sensitivity to immunotherapy, in a similar way as HRD is to PARPis, objective responses in cases with low TMB or non–HR-deficient tumors are not unusual (44, 45). Interestingly, a trend was observed between the number of mutations in genes included in the BROCA panel, which is considered a surrogate of HRDs, and a higher TMB. This association became significant when the analysis was restricted to *BRCA1* and *BRCA2*, the main genes responsible for the development of HRD gynecologic tumors. These results are in line with prior communications that have described higher DNA alterations and enriched immune infiltration in tumors with HRD (17). However, CPIs have not shown clear activity in tumors typically associated with HRD, like ovarian cancer (46).

The genomic stability of bladder cancer cells during treatment with the combination of an anti-PDL1 and a PARPi suggests that subsequent therapies should focus on targeting proteins like FAP, which is overexpressed after therapy, as shown in this study, or proteins constitutively present in bladder cancer, like nectin 4. Drugs targeting epigenetic processes could also be explored; conversely, searching for resistance mutations or developing targeted therapies against such mutations may be less attractive strategies.

In contrast to the genomic stability shown by WES, RNA-seq revealed a remarkable evolution of transcriptomic patterns during treatment. Twelve cancer hallmark signatures were enriched at cystectomy compared with TURBT. Interestingly, three of these patterns (EMT, inflammatory response, and TNFα signaling via NF-κB) were also overexpressed in nonresponders. EMT has been widely considered a predictor of poor prognosis and a resistance mechanism to both chemotherapy and immunotherapy (47–50). Thus, our data support the notion that targeting this molecular profile could improve the efficacy of immunotherapy, alone or in combination, and should be included in the molecular analysis of future studies. Regarding the TNFα via NF-κB category, it could be particularly interesting in this clinical context because, beyond its role in immune activation, NF-κB has been involved in *KRAS* oncogenic transformation (51). Though *KRAS* mutations are infrequent in bladder cancer, overexpression of pathways involving this gene in both posttreatment and

nonresponding samples could indicate a role as a mechanism of resistance. This could be especially interesting nowadays, when targeting KRAS has become a real option in some tumors (52).

On the other hand, the signatures "E2F targets" and "G2M checkpoint," identified as poor prognosis signatures in prior studies, were downregulated after treatment in our study population (53). Whether this repression could partially explain the significant pathologic response rate achieved by the combination of CPIs and PARPi remains speculative and should be confirmed in further studies. It is worth noting that the TGFβ signature was overexpressed at cystectomy. This finding is in line with previous studies that have established TGFβ as a key step in immune evasion and resistance to neoadjuvant immunotherapy (38, 53).

Also important, IFN-γ and IFN-α response signatures were upregulated in cystectomy samples and nonresponders. This conflicts with published data from the PURE01 trial, which assessed the efficacy of pembrolizumab alone as neoadjuvant treatment, in which both profiles were associated with a better response (3). Interestingly, these signatures played no role in a control cohort with chemotherapy. Thus, discrepancies could be due to the small sample size of both studies or the presence of olaparib in our combination. This highlights the importance of the clinical context when trying to understand the immune system and identify reliable markers of response.

Finally, our study did not show significant differences between immune cell populations at baseline and posttreatment samples nor when comparing responders versus nonresponders in peripheral blood. However, a trend toward higher levels of circulating CD4 T cells with undetectable levels of CD27 and CD28 was observed at all time points and became significant at follow-up. This cell subset has been reported to increase in the elderly and involves both effector memory T cells and terminal effector T cells (54, 55). Whether this population could lead to sustained disease control will be explored in future long-term analyses.

In summary, transcriptomic adaptations, rather than genomic modifications, determined resistance to neoadjuvant therapy with durvalumab and olaparib. Although these data should be properly validated, they should be considered when designing clinical trials or developing new drugs in this setting.

Authors' Disclosures

J.F. Rodríguez-Moreno reports grants, personal fees, and nonfinancial support from AstraZeneca during the conduct of the study, as well as grants, personal fees, and nonfinancial support from Bayer, Pierre Fabre, Regeneron, Bristol Myers Squibb, Novartis, Johnson & Johnson, and MSD, personal fees and nonfinancial support from Astellas and Pfizer, grants from Ipsen, and grants and personal fees from MERCK outside the submitted work, as well as employment at HM Hospitales and the Spanish Oncology Genito-Urinary Group. G. de Velasco reports personal fees from Astellas, Bristol Myers Squibb, Ipsen, AstraZeneca, Janssen, Bayer, MSD, Merck, Eisai, and Roche outside the submitted work. C. Álvarez-Fernández reports personal fees from Pfizer, Merck, Ipsen, Bayer, and AstraZeneca outside the submitted work. S. Vázquez reports grants from AstraZeneca during the conduct of the study, as well as grants from Bayer, Astellas, Bristol Myers Squibb, Ipsen, Roche, Janssen, and Pfizer outside the submitted work. P. Gajate reports other support from Bristol Myers Squibb, Merck, Roche, MSD, and Astellas outside the submitted work. A. Font reports grants from Roche and Astellas outside the submitted work. N. Lainez reports other support from AstraZeneca during the conduct of the study, as well as other support from Astellas, Bristol Myers Squibb, MSD, Merck, and Ipsen outside the submitted work. J. García-Donas reports grants from AstraZeneca during the conduct of the study, as well as grants and personal fees from Bristol Myers Squibb, AstraZeneca, Bayer, Astellas, Ipsen, Merck, MSD, Gilead, Novartis, Pharmamar, GlaxoSmithKline, Lilly, Pfizer, Roche, Janssen, and Piere Fabre outside the submitted work. No disclosures were reported by the other authors.

Authors' Contributions

J.F. Rodríguez-Moreno: Conceptualization, supervision, funding acquisition. **G. de Velasco:** Resources. **C. Álvarez-Fernández:** Resources. **R. Collado:** Resources. **R. Fernández:** Resources. **S. Vázquez:** Resources. **J.A. Virizuela:** Resources. **P. Gajate:** Resources. **A. Font:** Resources. **N. Lainez:** Resources. **E. Sevillano-Fernández:** Resources. **O. Graña-Castro:** Formal analysis. **L. Beltrán:** Formal analysis. **R. Madurga:** Formal analysis. **C. Rodríguez-Antona:** Methodology. **P. Berraondo:** Investigation. **S. Ruiz-Llorente:** Conceptualization, data curation, formal analysis, supervision, investigation, methodology, writing–original draft, writing–review and editing. **J. García-Donas:** Conceptualization, supervision, funding acquisition.

Acknowledgments

This study was sponsored by the Spanish Oncology Genitourinary Group and funded by an independent research grant from AstraZeneca. Neither the sponsor nor the funder had any role in data collection, data interpretation, or manuscript writing.

Note

Supplementary data for this article are available at Clinical Cancer Research Online (http://clincancerres.aacrjournals.org/).

Received September 18, 2024; revised December 20, 2024; accepted February 21, 2025; posted first April 29, 2025.

References

1. Grossman HB, Natale RB, Tangen CM, Speights VO, Vogelzang NJ, Trump DL, et al. Neoadjuvant chemotherapy plus cystectomy compared with cystectomy alone for locally advanced bladder cancer. N Engl J Med 2003;349:859–66.
2. Powles T, Catto JWF, Galsky MD, Al-Ahmadie H, Meeks JJ, Nishiyama H, et al. Perioperative durvalumab with neoadjuvant chemotherapy in operable bladder cancer. N Engl J Med 2024;391:1773–86.
3. Necchi A, Anichini A, Raggi D, Briganti A, Massa S, Lucianò R, et al. Pembrolizumab as neoadjuvant therapy before radical cystectomy in patients with muscle-invasive urothelial bladder carcinoma (PURE-01): an open-label, single-arm, phase II study. J Clin Oncol 2018;36:3353–60.
4. Powles T, Park SH, Voog E, Caserta C, Valderrama BP, Gurney H, et al. Avelumab maintenance therapy for advanced or metastatic urothelial carcinoma. N Engl J Med 2020;383:1218–30.
5. Galsky MD, Arija JÁA, Bamias A, Davis ID, De Santis M, Kikuchi E, et al. Atezolizumab with or without chemotherapy in metastatic urothelial cancer (IMvigor130): a multicentre, randomised, placebo-controlled phase 3 trial. Lancet 2020;395:1547–57.
6. Bellmunt J, de Wit R, Vaughn DJ, Fradet Y, Lee JL, Fong L, et al. Pembrolizumab as second-line therapy for advanced urothelial carcinoma. N Engl J Med 2017;376:1015–26.
7. Powles T, Csőszi T, Özgüroğlu M, Matsubara N, Géczi L, Cheng SY, et al. Pembrolizumab alone or combined with chemotherapy versus chemotherapy as first-line therapy for advanced urothelial carcinoma (KEYNOTE-361): a randomised, open-label, phase 3 trial. Lancet Oncol 2021;22:931–45.
8. Rose TL, Harrison MR, Deal AM, Ramalingam S, Whang YE, Brower B, et al. Phase II study of gemcitabine and split-dose cisplatin plus pembrolizumab as neoadjuvant therapy before radical cystectomy in patients with muscle-invasive bladder cancer. J Clin Oncol 2021;39:3140–8.
9. Funt SA, Lattanzi M, Whiting K, Al-Ahmadie H, Quinlan C, Teo MY, et al. Neoadjuvant atezolizumab with gemcitabine and cisplatin in patients with muscle-invasive bladder cancer: a multicenter, single-arm, phase II trial. J Clin Oncol 2022;40:1312–22.
10. Petrelli F, Coinu A, Cabiddu M, Ghilardi M, Vavassori I, Barni S. Correlation of pathologic complete response with survival after neoadjuvant chemotherapy in bladder cancer treated with cystectomy: a meta-analysis. Eur Urol 2014;65:350–7.

11. Pfister C, Gravis G, Fléchon A, Chevreau C, Mahammedi H, Laguerre B, et al. Dose-dense methotrexate, vinblastine, doxorubicin, and cisplatin or gemcitabine and cisplatin as perioperative chemotherapy for patients with nonmetastatic muscle-invasive bladder cancer: results of the GETUG-AFU V05 VESPER trial. J Clin Oncol 2022;40:2013–22.
12. Flaig TW, Tangen CM, Daneshmand S, Alva A, Lerner SP, Lucia MS, et al. A randomized phase II study of coexpression extrapolation (COXEN) with neoadjuvant chemotherapy for bladder cancer (SWOG S1314; NCT02177695). Clin Cancer Res 2021;27:2435–41.
13. Szabados B, Kockx M, Assaf ZJ, van Dam PJ, Rodriguez-Vida A, Duran I, et al. Final results of neoadjuvant atezolizumab in cisplatin-ineligible patients with muscle-invasive urothelial cancer of the bladder. Eur Urol 2022;82:212–22.
14. Westphalen CB, Fine AD, André F, Ganesan S, Heinemann V, Rouleau E, et al. Pan-cancer analysis of homologous recombination repair-associated gene alterations and genome-wide loss-of-heterozygosity score. Clin Cancer Res 2022;28:1412–21.
15. Lord CJ, Ashworth A. PARP inhibitors: synthetic lethality in the clinic. Science 2017;355:1152–8.
16. Börcsök J, Diossy M, Sztupinszki Z, Prosz A, Tisza V, Spisak S, et al. Detection of molecular signatures of homologous recombination deficiency in bladder cancer. Clin Cancer Res 2021;27:3734–43.
17. Yang C, Zhang Z, Tang X, Zhang X, Chen Y, Hu T, et al. Pan-cancer analysis reveals homologous recombination deficiency score as a predictive marker for immunotherapy responders. Hum Cell 2022;35:199–213.
18. Sen T, Rodriguez BL, Chen L, Corte CMD, Morikawa N, Fujimoto J, et al. Targeting DNA damage response promotes antitumor immunity through STING-mediated T-cell activation in small cell lung cancer. Cancer Discov 2019;9:646–61.
19. Rosenberg JE, Park SH, Kozlov V, Dao TV, Castellano D, Li JR, et al. Durvalumab plus olaparib in previously untreated, platinum-ineligible patients with metastatic urothelial carcinoma: a multicenter, randomized, phase II trial (BAYOU). J Clin Oncol 2023;41:43–53.
20. Vignani F, Tambaro R, De Giorgi U, Giannatempo P, Bimbatti D, Carella C, et al. Addition of niraparib to best supportive care as maintenance treatment in patients with advanced urothelial carcinoma whose disease did not progress after first-line platinum-based chemotherapy: the meet-URO12 randomized phase 2 trial. Eur Urol 2023;83:82–9.
21. Crabb SJ, Hussain S, Soulis E, Hinsley S, Dempsey L, Trevethan A, et al. A randomized, double-blind, biomarker-selected, phase II clinical trial of maintenance poly ADP-ribose polymerase inhibition with rucaparib following chemotherapy for metastatic urothelial carcinoma. J Clin Oncol 2023;41:54–64.
22. Powles T, Carroll D, Chowdhury S, Gravis G, Joly F, Carles J, et al. An adaptive, biomarker-directed platform study of durvalumab in combination with targeted therapies in advanced urothelial cancer. Nat Med 2021;27:793–801.
23. Grivas P, Loriot Y, Morales-Barrera R, Teo MY, Zakharia Y, Feyerabend S, et al. Efficacy and safety of rucaparib in previously treated, locally advanced or metastatic urothelial carcinoma from a phase 2, open-label trial (ATLAS). BMC Cancer 2021;21:593.
24. Sztupinszki Z, Diossy M, Krzystanek M, Reiniger L, Csabai I, Favero F, et al. Migrating the SNP array-based homologous recombination deficiency measures to next generation sequencing data of breast cancer. NPJ Breast Cancer 2018;4:16.
25. Kamoun A, de Reyniès A, Allory Y, Sjödahl G, Robertson AG, Seiler R, et al. A consensus molecular classification of muscle-invasive bladder cancer. Eur Urol 2020;77:420–33.
26. Chen B, Khodadoust MS, Liu CL, Newman AM, Alizadeh AA. Profiling tumor infiltrating immune cells with CIBERSORT. Methods Mol Biol 2018;1711:243–59.
27. Graña O, Rubio-Camarillo M, Fernández-Riverola F, Pisano DG, González-Peña D. Nextpresso: next generation sequencing expression analysis pipeline. Curr Bioinformatics 2018;3:583–91.
28. Trapnell C, Roberts A, Goff L, Pertea G, Kim D, Kelley DR, et al. Differential gene and transcript expression analysis of RNA-seq experiments with TopHat and Cufflinks. Nat Protoc 2012;7:562–78.
29. Langmead B, Trapnell C, Pop M, Salzberg SL. Ultrafast and memory-efficient alignment of short DNA sequences to the human genome. Genome Biol 2009;10:R25.
30. Li H, Handsaker B, Wysoker A, Fennell T, Ruan J, Homer N, et al. The sequence alignment/map format and SAMtools. Bioinformatics 2009;25:2078–9.
31. Frankish A, Diekhans M, Jungreis I, Lagarde J, Loveland JE, Mudge JM, et al. GENCODE 2021. Nucleic Acids Res 2021;49:D916–23.
32. Anders S, Pyl PT, Huber W. HTSeq–a Python framework to work with high-throughput sequencing data. Bioinformatics 2015;31:166–9.
33. Love MI, Huber W, Anders S. Moderated estimation of fold change and dispersion for RNA-seq data with DESeq2. Genome Biol 2014;15:550.
34. Subramanian A, Tamayo P, Mootha VK, Mukherjee S, Ebert BL, Gillette MA, et al. Gene set enrichment analysis: a knowledge-based approach for interpreting genome-wide expression profiles. Proc Natl Acad Sci U S A 2005;102:15545–50.
35. Liberzon A, Subramanian A, Pinchback R, Thorvaldsdóttir H, Tamayo P, Mesirov JP. Molecular signatures database (MSigDB) 3.0. Bioinformatics 2011;27:1739–40.
36. Newman AM, Steen CB, Liu CL, Gentles AJ, Chaudhuri AA, Scherer F, et al. Determining cell type abundance and expression from bulk tissues with digital cytometry. Nat Biotechnol 2019;37:773–82.
37. Cancer Genome Atlas Research Network. Comprehensive molecular characterization of urothelial bladder carcinoma. Nature 2014;507:315–22.
38. Powles T, Kockx M, Rodriguez-Vida A, Duran I, Crabb SJ, Van Der Heijden MS, et al. Clinical efficacy and biomarker analysis of neoadjuvant atezolizumab in operable urothelial carcinoma in the ABACUS trial. Nat Med 2019;25:1706–14.
39. Balar AV, Galsky MD, Rosenberg JE, Powles T, Petrylak DP, Bellmunt J, et al. Atezolizumab as first-line treatment in cisplatin-ineligible patients with locally advanced and metastatic urothelial carcinoma: a single-arm, multicentre, phase 2 trial. Lancet 2017;389:67–76.
40. Necchi A, Raggi D, Gallina A, Madison R, Colecchia M, Lucianò R, et al. Updated results of PURE-01 with preliminary activity of neoadjuvant pembrolizumab in patients with muscle-invasive bladder carcinoma with variant histologies. Eur Urol 2020;77:439–46.
41. Kelly T, Huang Y, Simms AE, Mazur A. Fibroblast activation protein-α: a key modulator of the microenvironment in multiple pathologies. Int Rev Cell Mol Biol 2012;297:83–116.
42. Marmouset V, Decroocq J, Garciaz S, Etienne G, Belhabri A, Bertoli S, et al. Therapy-related myeloid neoplasms following PARP inhibitors: real-life experience. Clin Cancer Res 2022;28:5211–20.
43. Merino DM, McShane LM, Fabrizio D, Funari V, Chen SJ, White JR, et al. Establishing guidelines to harmonize tumor mutational burden (TMB): in silico assessment of variation in TMB quantification across diagnostic platforms: phase I of the Friends of Cancer Research TMB Harmonization Project. J Immunother Cancer 2020;8:e000147.
44. Ledermann JA, Drew Y, Kristeleit RS. Homologous recombination deficiency and ovarian cancer. Eur J Cancer 2016;60:49–58.
45. Nero C, Ciccarone F, Pietragalla A, Duranti S, Daniele G, Salutari V, et al. Ovarian cancer treatments strategy: focus on PARP inhibitors and immune check point inhibitors. Cancers (Basel) 2021;13:1298.
46. McConkey DJ, Choi W, Marquis L, Martin F, Williams MB, Shah J, et al. Role of epithelial-to-mesenchymal transition (EMT) in drug sensitivity and metastasis in bladder cancer. Cancer Metastasis Rev 2009;28:335–44.
47. Amantini C, Morelli MB, Nabissi M, Cardinali C, Santoni M, Gismondi A, et al. Capsaicin triggers autophagic cell survival which drives epithelial mesenchymal transition and chemoresistance in bladder cancer cells in an Hedgehog-dependent manner. Oncotarget 2016;7:50180–94.
48. Casanova-Acebes M, Dalla E, Leader AM, LeBerichel J, Nikolic J, Morales BM, et al. Tissue-resident macrophages provide a pro-tumorigenic niche to early NSCLC cells. Nature 2021;595:578–84.
49. Dongre A, Rashidian M, Eaton EN, Reinhardt F, Thiru P, Zagorulya M, et al. Direct and indirect regulators of epithelial-mesenchymal transition-mediated immunosuppression in breast carcinomas. Cancer Discov 2021;11:1286–305.
50. Barbie DA, Tamayo P, Boehm JS, Kim SY, Moody SE, Dunn IF, et al. Systematic RNA interference reveals that oncogenic KRAS-driven cancers require TBK1. Nature 2009;462:108–12.
51. Skoulidis F, Li BT, Dy GK, Price TJ, Falchook GS, Wolf J, et al. Sotorasib for lung cancers with KRAS p.G12C mutation. N Engl J Med 2021;384:2371–81.
52. Wang Y, Chen L, Yu M, Fang Y, Qian K, Wang G, et al. Immune-related signature predicts the prognosis and immunotherapy benefit in bladder cancer. Cancer Med 2020;9:7729–41.
53. Batlle E, Massagué J. Transforming growth factor-β signaling in immunity and cancer. Immunity 2019;50:924–40.
54. Koch S, Larbi A, Derhovanessian E, Ozcelik D, Naumova E, Pawelec G. Multiparameter flow cytometric analysis of CD4 and CD8 T cell subsets in young and old people. Immun Ageing 2008;5:6.
55. Xu W, Larbi A. Markers of T cell senescence in humans. Int J Mol Sci 2017;18:1742.